Identification of a Submarine Fin-tip Vortex Using POD Analysis

Y. Xue[1, 2], C. Kumar[1], S.K. Lee[1], M. Giacobello[1], and P. Manovski[1]

[1] Defence Science & Technology Group, Victoria 3207, Australia

[2] Australian Maritime College, University of Tasmania, Tasmania 7248, Australia

Yunpeng.xue.2016@gmail.com

Abstract

The meandering nature of the fin-tip vortex generated by a manoeuvring submarine can lead to a smearing of the vortex in the ensemble-averaged flow field. From stereoscopic particle image velocimetry (SPIV) measurements, it is possible to remove the smearing by shifting each instantaneous velocity field so as to produce a common centre for the vortex. However, it is difficult to identify the instantaneous vortex centre due to the presence of measurement noise and strong small-scale turbulent fluctuations. In this paper, a snapshot Proper Orthogonal Decomposition (POD) technique is used to capture the dominant large-scale coherent structures (from inspection of eigenvalue or energy distributions) to improve vortex identification and subsequent correction for meandering. The present findings suggest that, for the flow fields reconstructed from POD and subsequently corrected for meandering, the vortex flow exhibits steeper velocity gradients and is less noisy than the original results (inspection shows the reduction in turbulent fluctuation is as much as 16%).

Introduction

The terms vortex core meandering, vortex core wandering or vortex core precession are used to describe the instability of a swirling flow which is a time-dependent flow pattern, where the core of the system oscillates around the rotational axis. This phenomenon of the vortex instability exists in both open flow, such as wing-tip vortex wandering [1], and confined flow, such as vortex core precession in vortex tube [2] and vortex flow solar reactor [3]. The behaviour of vortex meandering/wandering or precession is of general interest because it can affect the transport of momentum and energy of the working fluid. For this paper, the interest is particularly on the meandering of an open-flow vortex trailing from the bridge fin-tip of a generic conventional submarine [4, 5] using different vortex identification criteria. The bridge fin-tip vortex is a major flow feature produced on the upper hull of the submarine during a pitch or yaw manoeuvre, and it can impact on the acoustic signature. Clarification of the meandering effect is important in the validation of the high-fidelity computational models.

The submarine geometry under consideration is known as the 'BB2' [5], which consists of an axisymmetric body with a casing, a bridge fin and control surfaces. Recently, a model scale of this geometry was built to allow stereoscopic particle image velocimetry (SPIV) testing of the model at 10° yaw in the Low-Speed Wind Tunnel at Defence Science and Technology (DST) Group [5]. The model has a length (L) of 2 m and a length-to-diameter ratio of 7.3. On the casing, the shape of the bridge fin is that of NACA-0022 with a height of 8%L and a chord length of 15.7%L. A nominal free stream velocity of 29 m/s was set resulting in a model-length Reynolds number of 4×10^6 (chord-length Reynolds number of 0.63×10^6). SPIV measurements have been conducted to obtain the 3-D velocity profiles at three selected measurement planes along with the model (51.1%L, 65.0%L and 81.5%L); see Figure 1. For

further details on the submarine geometry, wind tunnel configuration, SPIV setup and parameters, and data processing, see [5].

The instantaneous SPIV measurements allow the possibility of shifting the image sequence to a common vortex core centre and effectively eliminating the meandering effect from the ensemble average and the flow statistics, which are important to characterise the flow field and hence to identify the impacts of the fin-tip vortex meandering.

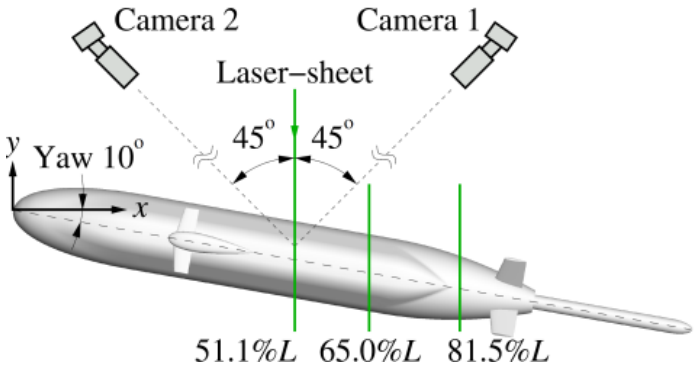

Figure 1. The BB2 generic conventional submarine model at 10° yaw and the SPIV measurement planes.

Proper Orthogonal Decomposition and Reconstruction

The objective is achieved by using a snapshot Proper Orthogonal Decomposition (POD) technique to capture the dominant large-scale coherent structure to improve vortex identification which then allows correction for meandering. The left image of Figure 2 is an instantaneous velocity field of the bridge fin-tip vortex at 65%*L,* which is the only measurement plane analysed in the current work. The noise or incoherent small-scale turbulent structures presented in the figure highlights the difficulty in the identification of the dominating turbulent structure and the vortex core. POD has been found to be effective in decomposing complex turbulent flow into a set of modes that represents the dominating flow structures [1, 6, 7].

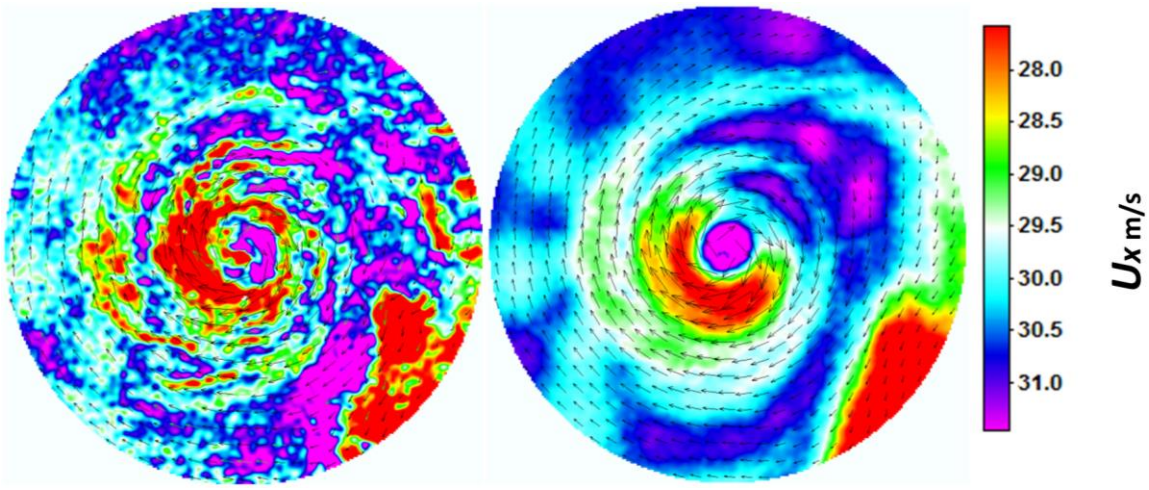

Figure 2. Left: an instantaneous velocity field of the bridge fin-tip vortex at 65% of the model length. Right: reconstruction of the same instantaneous velocity field based on the first three modes from the POD analysis. The contour levels represent the out-of-plane streamwise velocity (U_x).

The elementary idea of POD is to define a set of orthogonal functions (eigenmodes) with coefficients representing the flow field based on an energy-weighted calculation (eigenvalue or energy level). It is subsequently possible to identify the dominating large-scale coherent

structures that contribute the most energy to the flow. Reconstruction of the velocity vector field using only the most energetic modes enables the dominant structures of the flow to be more clearly captured and improves the identification of the vortex core. Mode information of the snapshot POD and its mathematical process can be found in previous publications [1, 6, 7].

Instead of the POD analysis being applied to the whole velocity field of each measurement plane as presented in [5], the bridge fin-tip vortex (which includes the vortex and some wake component) and the vortex core are selected for accurate POD analysis. The centre of the bridge fin-tip vortex has been identified by the minimum the local out-of-plane vorticity (ω_x) with the normalized centre coordinates given in [5]. The fin-tip vortex and the vortex core are defined by the swirl velocity distribution as presented in Figure 3. A 30% of the maximum swirl velocity is selected to separate the fin-tip vortex ($D_{30\%Uy,\ max}$) from the whole velocity field and the forced vortex part within the central region is defined as the vortex core ($D_{vortex\ core}$). The diameter of the vortex core is about 0.01*L*, which is in a good agreement with the turbulent intensity defined vortex core in [5].

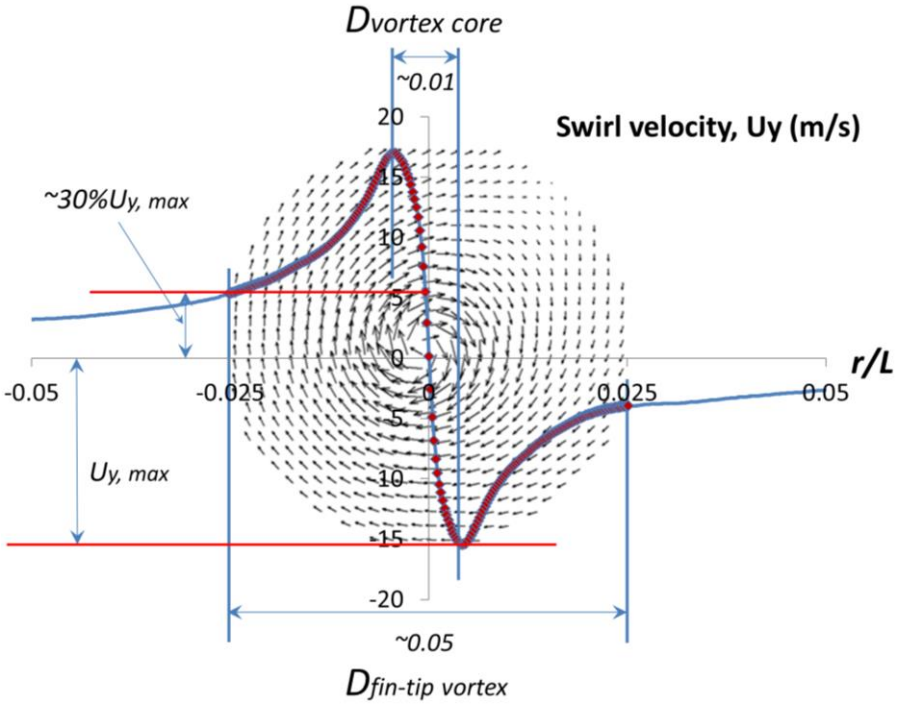

Figure 3. Swirl velocity distribution across the bridge fin-tip vortex and the selected views for POD analysis.

To perform the POD analysis efficiently, 1000 snapshots out of the available 3000 instantaneous velocity fields were used. Figure 4 presents the contributions from the POD modes to the total turbulent kinetic energy (energy level) in three configurations, i.e., 1000 snapshots of the bridge fin-tip vortex, 3000 snapshots of the bridge fin-tip vortex and 1000 snapshots of the vortex core. It can be seen from the figure that the lower modes contain most of the energy, while the contributions from the higher modes (≥5) are negligible for both the fin-tip vortex and the vortex core.

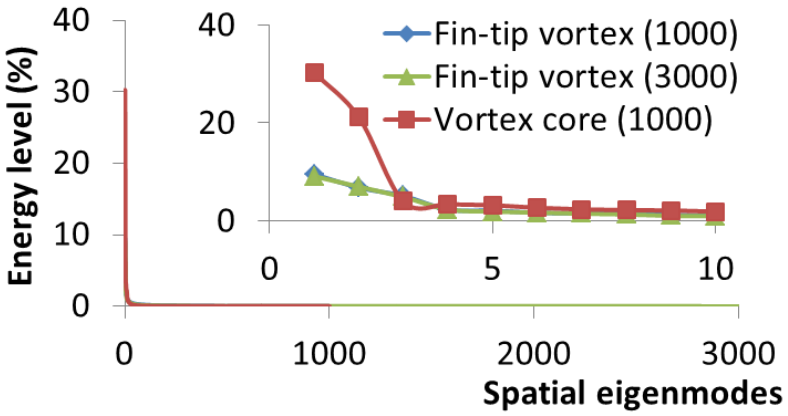

Figure 4. Contributions from the POD eigenmodes to the total energy for different cases with a particular focus on the first ten modes (1000 snapshots of the bridge fin-tip vortex, 3000 snapshots of the bridge fin-tip vortex and 1000 snapshots of the vortex core).

There is a maximum of 3% difference of the eigenvalues between the 1000 and the 3000 snapshots cases. This confirms the accuracy and acceptance of the POD analysis using 1000 snapshots of the vector fields instead of the 3000 vector fields. All the other POD analysis in this current work is based on the 1000 snapshots. Furthermore, the eigenvalues of the first three modes of the fin-tip vortex, i.e., 9.5%, 6.8%, and 5.1%, respectively, indicate the existence of dominating large-scale coherent turbulent structures compared to the remaining eigenmodes. The greater eigenvalues of the vortex core (30.3% and 21.1%) show more significant dominating large-scale coherent turbulent structures with the first two modes containing about 51.4% of the total turbulent kinetic energy (TKE). The difference of the eigenvalue distribution is due to the different regions selected for the POD analysis. For the selected bridge fin-tip vortex region, some small scale turbulent structures in the fin wake are included, while it is pure vortex flow in the selected vortex core region.

An instantaneous velocity field of the vortex core, the first three POD modes of the selected velocity vector and the reconstruction of the flow field based on the first three modes are presented in Figure 5. The two most energetic modes mainly consist of two counter-rotating vortex pair and owing to the symmetry along the axis of the mean flow; mode 2 is obtained from mode 1 by a 90 degree rotation. This is in good agreement with the POD analysis of a vortex flow in a cylinder duct [8] and the POD analysis of a wing-tip vortex in an open field [9]. Based on the most energetic modes, the velocity field can be reconstructed as shown in the figure which shows a clearer view of the velocity field. Figure 2 (right) shows the reconstruction of the same instantaneous velocity field (left) based on the first three modes from the POD analysis. The same improvement of the selected view is also seen from the top two images in Figure 5. Comparing with the original image, the small-scale fluctuations have been removed providing a much clearer view of the vector field, which will enable accurate identification of the dominating flow structure and location of the vortex centre.

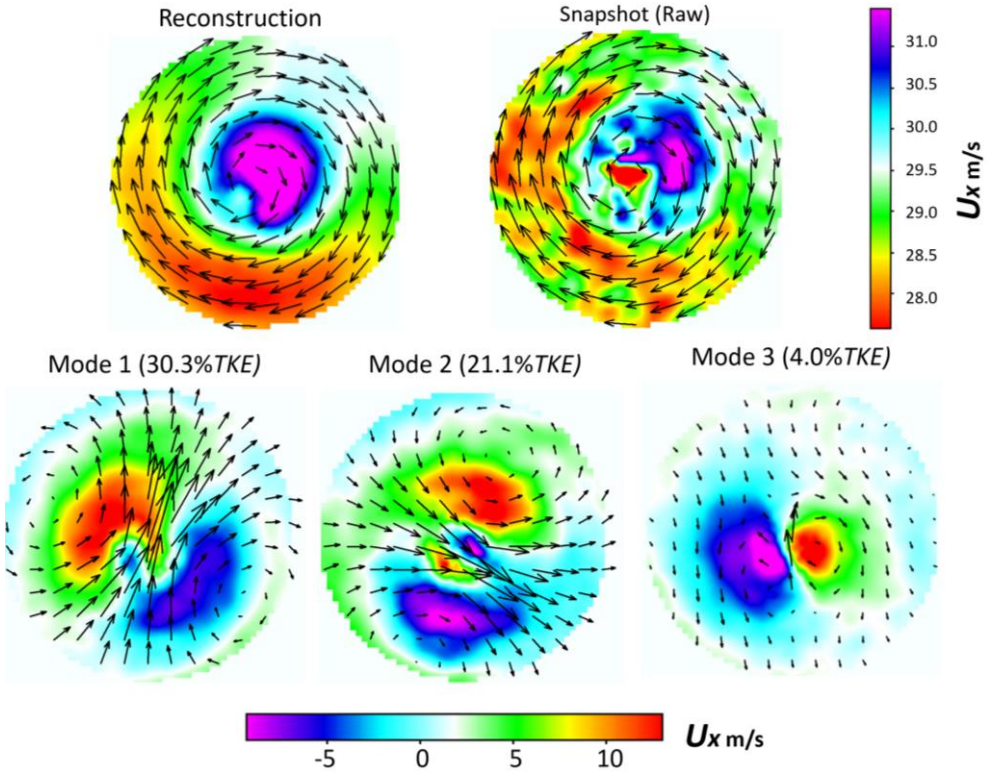

Figure 5. Top: an instantaneous velocity field of the vortex core and the reconstruction of the flow field based on the first three modes. Bottom: first three POD modes with their eigenvalues/energy level.

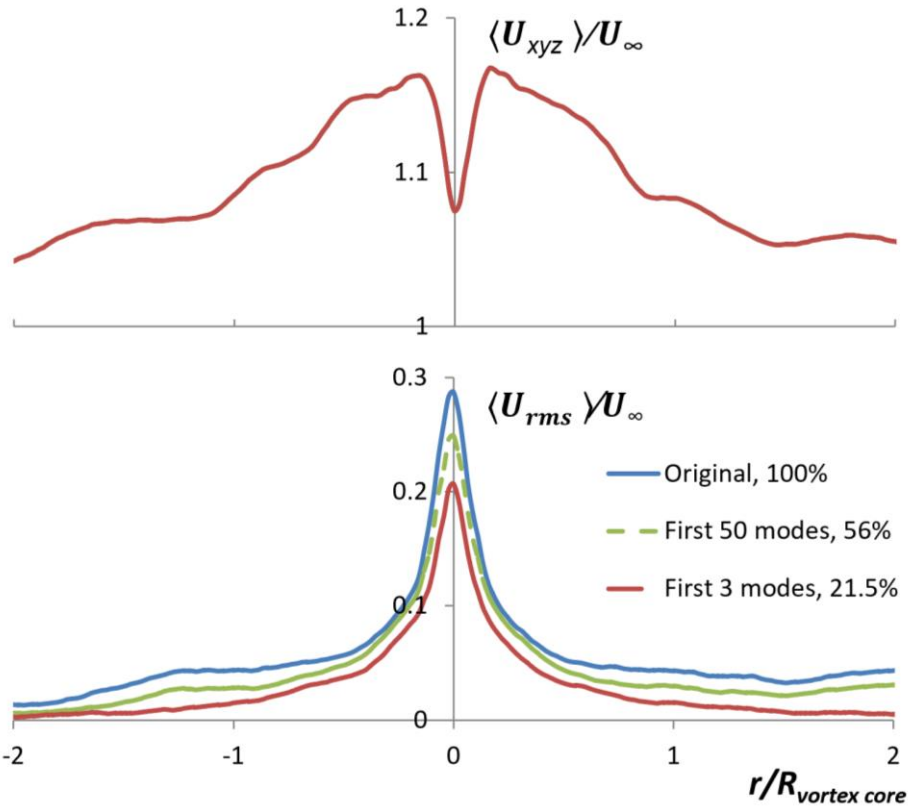

Figure 6. The normalized resultant velocity and the turbulence intensity of the original raw data, the POD approximation (first 50 modes, 56% of total turbulent energy) and the POD approximation (first 3 modes, 21.5% of total turbulent energy at 65%*L*.

Before further analysis of the bridge fin-tip vortex, assessment of the POD results is conducted. Figure 6 presents the normalized resultant velocity and fluctuating components (fin-tip vortex) averaged using the original velocity field, the approximated velocity field based on the first 50 modes of the POD analysis and the approximation based on the first three modes. It is clearly seen that the reconstructed average velocity field has no change from the original value and is independent of the modes used in the approximation. While, the significant impact of the POD approximation on smoothing the velocity field as shown in Figure 2 and Figure 5 is achieved by removing the small scale turbulent structure. Of course, the original velocity field has 100% of the turbulent energy, and the approximations based on the first 50 and 3 modes contain 56% and 21.5% of the total turbulent energy, respectively. With a decrease of the modes used in the reconstruction, the turbulence intensity drops significantly. The more modes used, the more turbulent energy will be kept and the more accurate approximation will be obtained, but the identification of the dominating flow structure will be more difficult. The characteristics of POD is that it does not change the average flow field but only impacts the turbulent components and therefore makes it a good pre-processing technique for further analysis.

Vortex core meandering correction

As mentioned above, the minimum local out-of-plane vorticity (obtained using a second order central finite difference scheme) is used to locate the vortex centre in the current work and in [5]. The 1000 snapshots of the vortex core defined in Figure 3 are used to analyse the meandering of the fin-tip vortex. A probability density function (PDF) of the instantaneous vortex centre of the 1000 selected raw and POD-corrected velocity fields are plotted in Figure 9.

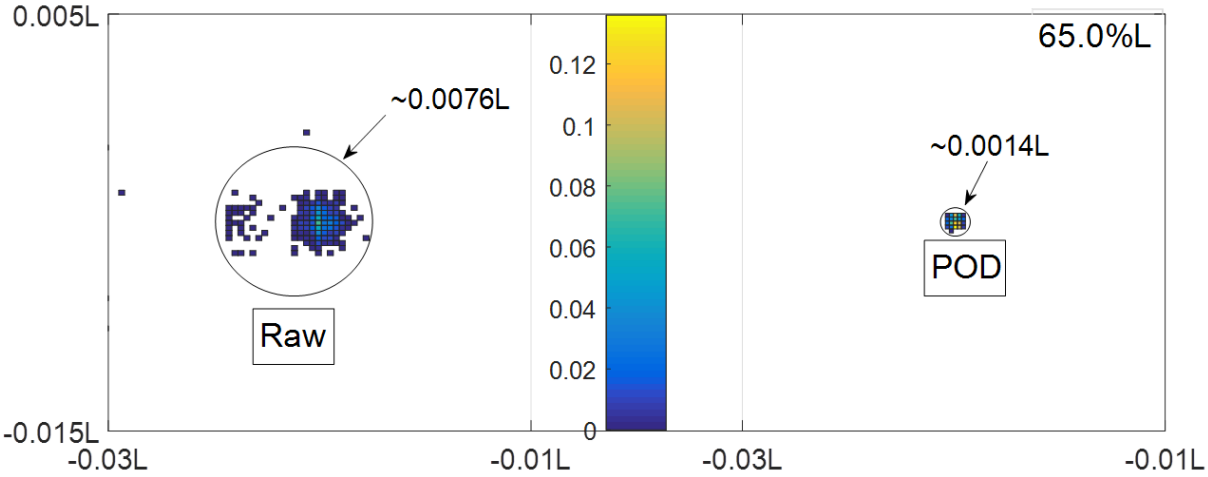

Figure 7. Probability density function (PDF) of the instantaneous vortex centre of the raw and POD-corrected velocity vectors identified by the minimum vorticity at three axial locations along the model.

The relative location of the instantaneous vortex centre can be seen from the figure and its probability density is indicated by the colour bar. The actual location of the vortex centre from the ensemble average velocity field is presented in [5]. A significant decrease of the vortex meandering area can be seen after each image sequence is shifted to a common vortex centre using POD (diameter of the estimated meandering area is indicated in the figure). The concentrated vortex centres found in the POD approximated velocity fields indicate the area that meandering occurs. The vortex centre that locates outside of the main cluster of the raw data should be considered as false results caused by the noise in the instantaneous velocity

vectors. The secondary meandering centre of the vortex core that is indicated by the smaller cluster of the concentrated vortex centre away from the main region should also be considered as a result of the noise or small scale turbulent structure.

With the identified centre of the vortex core, the instantaneous velocity vectors are shifted to be coincident with the vortex centre in each vector field. In such a way, the effects of the vortex meandering on the flow field are removed and the meandering corrected velocity vectors are compared with the original results. The ensemble averaged resultant velocity (U_{xyz}) and fluctuation components (U_{rms}) for four cases are normalized using the free stream velocity and presented in Figure 8.

The 'Raw' and 'POD (3 modes)' are the raw data and the POD approximation using the first three modes. The 'Raw corrected' refers to the raw data corrected based on the vortex centre identified by the raw velocity field. The 'POD & Meandering corrected (PM)' refers to the meandering corrected using POD approximation. The 'Raw & Meandering corrected using POD (RM)' is the raw data processed in the following steps:

1. Use the vorticity to identify the vortex centre of the POD reconstructed velocity fields (first three modes);
2. Shift the raw velocity vector fields using these centre coordinates to remove the meandering effect;
3. Obtain the normalized ensemble-averaged velocity and turbulence intensity of the meandering corrected raw data.

The three meandering corrected resultant velocity results (Raw corrected, PM and RM) show an increased maximum velocity (~1%) at about $|r/L|=1.556\times10^{-3}$ and decreased velocity at the centre of the vortex (~3.7%). This sharpening and narrowing effect of the meandering corrected resultant velocities comparing to the raw and POD corrected cases is a result of the elimination of the meandering effect.

Comparing to the raw data, the normalized turbulence intensity ($\langle U_{rms}\rangle/U_\infty$) of the POD approximation shows an even drop across the vortex core, which is caused by removing the small-scale incoherent turbulent structure and measurement noise. Further removal of the meandering effect from the POD approximation (RM) results in a significant weakening of the fluctuation. The decrease of the flow fluctuation from the raw to the POD approximated and then to the POD and meandering corrected data implies the turbulence of the original vortex core mainly consists of two components, i.e., the incoherent turbulent and the fluctuation induced by the meandering. The maximum fluctuation in the PM case is about 0.1 and only consists of the fluctuation from the first three dominating modes. All the small scale turbulence and meandering induced turbulence are removed. The 'Raw and Meandering corrected using POD' case also has a significant drop in the central region (16.1%) and this decrease of the fluctuation is getting smaller in the outer region of the vortex core. The peak fluctuating core region is defined as $\langle U_{rms}\rangle/U_\infty \leq 0.1$. A significant decrease of this region is observed after the correction of meandering, i.e., from 0.44 $D_{vortex\ core}$ to 0.26 $D_{vortex\ core}$. While, the 'Raw corrected' method shows a higher fluctuation in most part of the vortex core and this increased fluctuation is observed in all configurations. A bimodal peak in the central region is also observed here, which is likely a result of the false centre due to small scale turbulence, measurement noise and 'holes'.

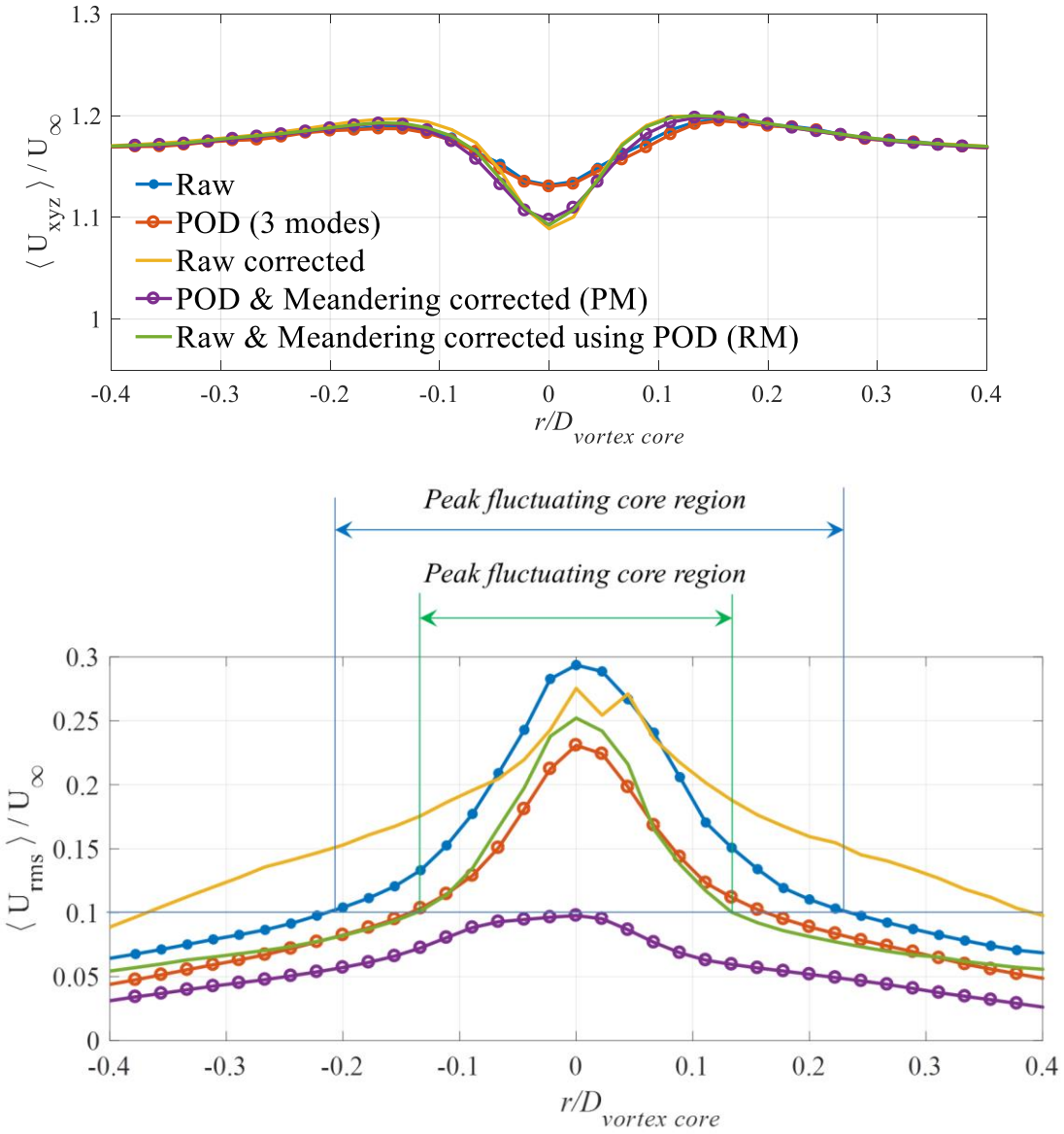

Figure 8. The normalized resultant velocity and fluctuation of Raw, POD approximated, raw corrected, POD & Meandering corrected and Raw & Meandering corrected using POD results at 65.0%L.

Several other local vortex identification criteria are also used in the current work, including the out-of-plane velocity (U_x), the Q criterion, Lambda-2 criterion (λ_2) and Gamma-1 criterion (Γ_1). The detail definitions of these criteria can be found in [11-13]. The normalized resultant velocity and fluctuation of raw data and meandering corrected results using different vortex identification criteria are presented in Figure 9. The vortex meandering is corrected with the vortex centre identified from POD processed data. It can be concluded from the plot of resultant velocity (U_{xyz}) that all criteria give similar results.

The bottom plot of Figure 9 is the meandering corrected fluctuation using different criteria with the vortex centre identified by the POD reconstructed velocity vector fields. It highlights a good agreement of the fluctuations corrected using different criteria, while the slight difference of the Γ-1 criterion is due to the different identified vortex centre. This means, for noisy or highly turbulent data, a POD reconstruction is necessary for the identification of the vortex centre and all gradient-based vortex identification criteria tested here can result in accurate identification of the vortex centre based on the POD reconstructed velocity fields.

The decrease of the fluctuating component after correcting the meandering confirms the contribution of the vortex meandering to the total fluctuation.

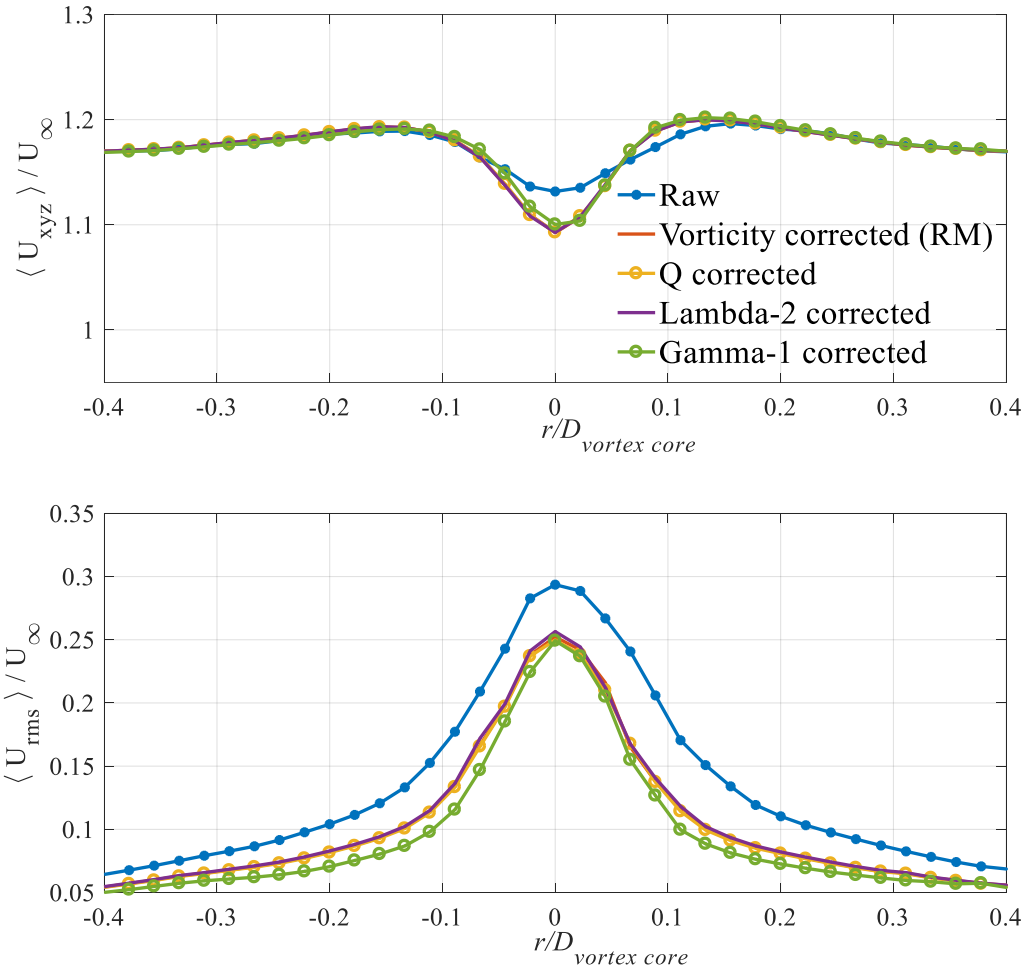

Figure 9. The normalized resultant velocity and fluctuation of raw data and meandering corrected results using different vortex identification criteria at 65.0%L.

Conclusion and recommendation

This paper presented a study of a submarine bridge fin-tip vortex using recently acquired SPIV measurements [5] from the DST Low-Speed Wind Tunnel. The vortex flow is analysed using a snapshot POD technique to establish the dominant large-scale turbulent structure. Several local vortex identification criteria were used to identify the vortex centre in the raw vortex field and POD reconstructed velocity field.

It is found the POD reconstruction of the velocity field can significantly improve the accuracy of the vortex centre identification, especially with the PIV measurement result that contains measurement noise, small scale turbulence, and missing data in the core region. For the POD reconstructed velocity vector fields, all criteria can generate a cleaner view to identify the vortex centre and the flow characteristics after meandering corrections have a good agreement. It is found that the vortex meandering has little impact on the ensemble-averaged resultant velocity with a maximum difference of 3.7%, but a significant influence on the fluctuating component with a reduction in the central region up to 16.1%. The meandering correction also leads to a significant decrease of the peak fluctuating core region.

Overall, this work serves as an initial step towards understanding the meandering nature of the fin-tip vortex. Another possibility is to extend the work to include time-resolved measurements to identify the frequency of vortex meandering. To obtain good measurement results in the core region of a gaseous vortex flow, neutrally buoyant tracer, such as helium-filled soap bubble, is recommended in the optical measurement.

Acknowledgement

The authors acknowledge the support and funding of DST's Maritime Division as well as the support of the Research Training Centre of Naval Design and Manufacturing (RTCNDM). The RTCNDM is a University-Industry partnership established under the Australian Research Council (ARC) Industry Transformation grant scheme (ARC IC140100003).

Reference

[1] A. Chatterjee, "An introduction to the proper orthogonal decomposition," Current Science, Article vol. 78, no. 7, pp. 808-817, 2000.

[2] X. Guo and B. Zhang, "Computational investigation of precessing vortex breakdown and energy separation in a Ranque–Hilsch vortex tube," International Journal of Refrigeration, Article vol. 85, pp. 42-57, 2018.

[3] A. Chinnici, Y. Xue, T. C. W. Lau, M. Arjomandi, and G. J. Nathan, "Experimental and numerical investigation of the flow characteristics within a Solar Expanding-Vortex Particle Receiver-Reactor," Solar Energy, vol. 141, pp. 25-37, 1/1/ 2017.

[4] C. Fureby et al., "Experimental and numerical study of a generic conventional submarine at 10° yaw," Ocean Engineering, vol. 116, no. Supplement C, pp. 1-20, 2016/04/01/ 2016.

[5] S. K. Lee, P. Manovski, and C. Kumar, "Wake of a DST Submarine Model captured by Stereoscopic Particle Image Velocimetry," in 21th Australasian Fluid Mechanics Conference, Adelaide, Australia, 2018.

[6] G. Berkooz, P. Holmes, and J. L. Lumley, "The proper orthogonal decomposition in the analysis of turbulent flows," in Annual Review of Fluid Mechanics vol. 25, ed, 1993, pp. 539-575.

[7] L. Sirovich, "Turbulence and the dynamics of coherent structures. I. Coherent structures," Quarterly of applied mathematics, vol. 45, no. 3, pp. 561-571, 1987.

[8] L. Graftieaux, M. Michard, and N. Grosjean, "Combining PIV, POD and vortex identification algorithms for the study of unsteady turbulent swirling flows," Measurement Science and technology, vol. 12, no. 9, p. 1422, 2001.

[9] A. Dahmouni, M. Oueslati, and S. B. Nasrallah, "Experimental Investigation of Tip Vortex Meandering in the Near Wake of a Horizontal-Axis Wind Turbine," Journal of Applied Fluid Mechanics, vol. 10, no. 6, pp. 1679-1688, 2017.

[10] A. M. Edstrand, T. B. Davis, P. J. Schmid, K. Taira, and L. N. Cattafesta, "On the mechanism of trailing vortex wandering," Journal of Fluid Mechanics, vol. 801, p. R1, 2016, Art. no. R1.

[11] J. Jeong, and F. Hussain, "On the identification of a vortex", Journal of fluid mechanics, 285: p. 69-94,1995.

[12] V. Kolář, "Vortex identification: New requirements and limitations," International journal of heat and fluid flow, 28(4): p. 638-652, 2007.

[13] Y. Zhang, et al., "A review of methods for vortex identification in hydroturbines," Renewable and Sustainable Energy Reviews, 2017. 81(1): p. 1269-1285.